AMEGHINIANA
A GONDWANAN PALEONTOLOGICAL JOURNAL

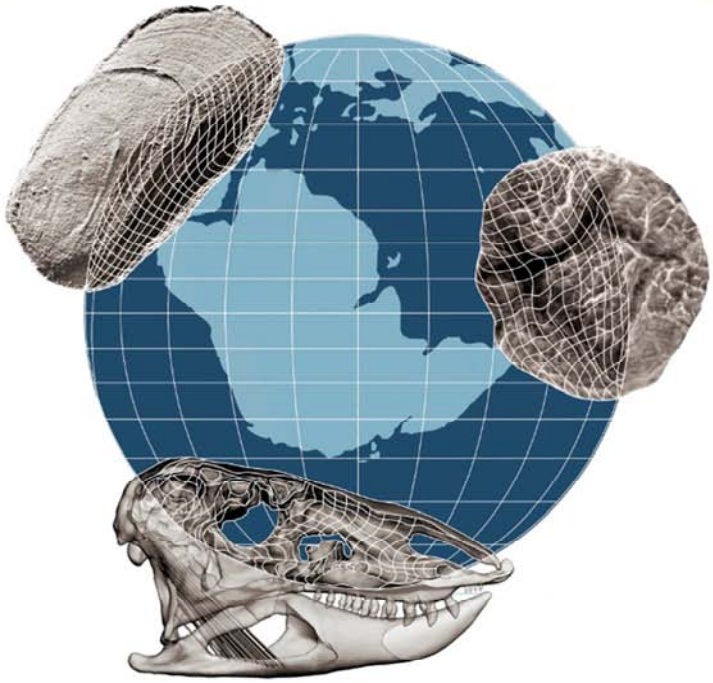

Submitted: 21 June 2022 - **Accepted**: 2 March 2023 - **Posted online**: 10 March 2023

To link and cite this article:

doi: 10.5710/AMGH.02.03.2023.3525

MAASTRICHTIAN MICROFOSSILS OF THE SHALLOW MARINE UMIR FORMATION, NORTHEASTERN COLOMBIA

MICROFÓSILES DEL MAASTRICHTIANO EN AMBIENTES MARINOS SOMEROS DE LA FORMACIÓN UMIR (NORESTE DE COLOMBIA)

GERMAN D. PATARROYO[1,2], KARLOS G.D. KOCHHANN [1,2], RODRIGO M. GUERRA [2,3], LAIA ALEGRET[4], DAIANE CEOLIN [2], AND JOSÉ M. TORRES[5]

[1]Programa de Geologia, Universidade do Vale do Rio dos Sinos, Avenida Unisinos, 950, CP 93.022-970 São Leopoldo, RS, Brazil. germanp@edu.unisinos.br

[2]Technological Institute for Paleoceanography and Climate Change (itt Oceaneon), UNISINOS University, 950, CP 93.022-970 São Leopoldo, RS, Brazil. kkochhann@unisinos.br; rmguerra@unisinos.br; daiaceolin@unisinos.br

[3]Museu Itinerante de Ciências Naturais. CP 95.185-000, Carlos Barbosa, RS, Brazil.

[4]Dept. Ciencias de la Tierra & IUCA, Universidad de Zaragoza. Pedro Cerbuna 12, 50009 Zaragoza, Spain. laia@unizar.es

[5]Department of Earth and Environment, Florida International University, 11200 SW 8th St, Miami, FL, USA. manutorresgeo@gmail.com

38 pag. (text + references); 6 figs.; 3 tables

Running Header: PATARROYO *ET AL.*: MAASTRICHTIAN MICROFOSSILS FROM COLOMBIA

Short Description: Marine microfossils (foraminifers, calcareous nannofossils, ostracods) recorded a gradual shallowing trend in the Umir Formation (northern Colombia) during the Maastrichtian.

Corresponding author: German David Patarroyo Camargo; germanp@edu.unisinos.br

Abstract. During the Late Cretaceous, northern South America was characterized by broad epicontinental seas, with variable surface productivity and changing bottom-water oxygenation. However, global sea-level fluctuations and local tectonic shifts caused their disappearance in the latest Cretaceous. We present an integrated micropaleontological (foraminifers, calcareous nannofossils, ostracods) and geochemical study of a section comprising the Umir Formation and its lower stratigraphic contact with the La Luna Formation, in the Middle Magdalena Valley (MMV), northeastern Colombia. Foraminiferal assemblages were moderately diverse and mainly dominated by benthic taxa, characterizing the local assemblage biozones *Siphogenerinoides bramlettei* and *Ammobaculites colombiana* (Maastrichtian). Planktonic foraminiferal assemblages were less diversified, being species assigned to Heterohelicidae and scarce keeled forms (*Globotruncana* spp.) the most recurrent taxa. Ostracod recovery was very scarce, and we could only identify the genus *Actinocythereis*. In contrast, calcareous nannofossil assemblages were moderately diversified along the section, and composed of typical Late Cretaceous low-latitude taxa such as *Micula staurophora*, *Cribrosphaerella ehrenbergii*, *Gartnerago segmentatum*, among others. The identified microfossils generally indicate a transition from middle-inner shelf conditions, with moderately oxygenated bottom waters within the La Luna Formation, to a shallower marine setting within the Umir Formation. This interpretation is supported by Sr/Ba and log(Fe/Ca) ratios measured in bulk sediment, which indicate increased continental runoff and terrigenous input in the upper part of the section. Moreover, a significant biotic turnover was identified at the base of the section, suggesting the presence of a xenoconformity at the La Luna-Umir stratigraphic contact. The xenoconformity between those units has been previously described and proposed as a regional stratigraphic feature.

Keywords. Paleoenvironments. Late Cretaceous. Colombia. Micropaleontology.

MICROFÓSILES DEL MAASTRICHTIANO EN AMBIENTES MARINOS SOMEROS DE LA FORMACIÓN UMIR (NORESTE DE COLOMBIA)

El Cretácico Tardío del norte de América del Sur estuvo dominado por mares epicontinentales de gran extensión, con fluctuaciones de la productividad superficial y la oxigenación en los sedimentos de fondo. Sin embargo, cambios en los regímenes tectónicos locales y descensos globales en el nivel del mar, llevaron a la desaparición de dichos ambientes hacia el Cretácico terminal.

Se presentan los resultados del estudio micropaleontológico (foraminíferos, nanofósiles calcáreos, ostrácodos) y geoquímico en una localidad de la Formación Umir y su contacto basal con la Formación La Luna en el Valle Medio del Magdalena (VMM), nororiente de Colombia. Las asociaciones de foraminíferos fueron principalmente formas bentónicas moderadamente diversas, que definen las biozonas de asociación locales *Siphogenerinoides bramlettei* y *Ammobaculites colombiana* (Maastrichtiano). Las formas planctónicas, menos diversas, comprenden ejemplares de Heterohelicidae y escasas formas quilladas (*Globotruncana* spp.). El registro de ostrácodos fue muy escaso, comprendiendo el género *Actinocythereis*. En contraste, las asociaciones de nanofósiles calcáreos fueron moderadamente diversas y comprendieron formas típicas de bajas latitudes del Cretácico Tardío como *Micula staurophora*, *Cribrosphaerella ehrenbergii*, *Gartnerago segmentatum*, entre otras.

En general, las asociaciones de microfósiles indican una transición de condiciones de plataforma interna a media, moderadamente oxigenada en la Formación La Luna, hacia un entorno más restringido en la Formación Umir. Esta interpretación es corroborada por las relaciones de Sr/Ba y log(Fe/Ca) de las muestras de roca estudiadas, las cuales indican un aumento en el aporte de terrígenos vía escorrentía continental hacia la parte

superior de la sección. De igual forma, la variación significativa en las asociaciones de microfósiles hacia la base sugiere la presencia de una xenoconformidad en el contacto La Luna-Umir. Dicha xenoconformidad ha sido previamente reportada como de carácter regional.

Palabras clave. Paleoambientes. Cretácico Tardío. Colombia. Micropaleontología.

NORTHERN SOUTH AMERICA underwent a series of geological reorganizations at the end of the Mesozoic era. For instance, the onset of the Andean orogeny likely occurred during the Campanian-Maastrichtian, causing significant shifts of regional sedimentary regimes, in progressively shallowing widespread epicontinental seas, with high surface productivity and the occurrence of recurrent anoxic episodes (Martinez and Hernandez, 1992; Villamil and Pindell, 1998; Erlich et al., 1999; Sarmiento-Rojas, 2019; Montes et al., 2019; Bayona et al., 2020). In addition, the latest Cretaceous was characterized by a global sea-level fall, which has been associated with the possible occurrence of intermittent ice sheets at high latitudes (Hardenbol et al., 1998; Kominz et al., 2008; Huber et al., 2018). Consequently, Campanian-Maastrichtian sedimentary successions of northern South America record a myriad of tectonic (basin deformation, local uplifts), stratigraphic (xenoconformities, diachronism of units), and sedimentary (abrupt lateral facies shifts, retrogradational stacking) features that make their depositional evolution highly complex (Ayala-Calvo et al., 2009; Bayona et al., 2011, 2020; Sarmiento et al., 2015; Montaño et al., 2016; Sarmiento-Rojas, 2019; Terraza, 2019; Valencia-Gómez et al., 2020; Gramal-Aguilar et al., 2021).

Marine microfossils have enabled paleoenvironmental reconstructions and chronostratigraphic constraints of the Upper Cretaceous sedimentary successions of northern South America (Bürgl and Dummit, 1954; Petters, 1955; Sole de Porta, 1972; Martínez, 1989, 2003; Sarmiento, 1992; Vergara, 1997; Guerrero et al., 2000; Yepes, 2001; Tchegliakova and Mojica, 2001; Garzón et al., 2012; Patarroyo et al., 2017, 2022; Carvalho et al., 2021; De La Parra et al., 2022). This is the case for the Maastrichtian Umir Formation, cropping out in the Middle Magdalena Valley (MMV), northeastern Colombia (Fig. 1), where depositional and chronostratigraphic interpretations have been traditionally based on microfossils, and eventually, integrated with sedimentological

studies (Tchegliakova, 1993, 1995, 1996; Santos, 2012; Montaño et al., 2016; Navarrete et al., 2018; Terraza, 2019). However, since most of these studies have focused on economically relevant coal-bearing strata of the middle and upper part of this unit, there is still debate on whether the lower part of the Umir Formation was deposited in a marine setting, and on the nature of its boundary with the underlying La Luna Formation. Previous works suggested the presence of an unconformity or a condensed section between the La Luna and Umir formations, as well as in coeval units in more proximal areas, such as in the Catatumbo and Cesar-Rancheria basins (Ward et al., 1973; Sarmiento et al., 2015; Terraza, 2019).

Here we present a micropaleontological (foraminifers, ostracods, and calcareous nannofossils) and geochemical (sediments elemental ratios) survey for a stratigraphic section that spans the lowermost segment of the Umir Formation (Maastrichtian) and its contact with the underlying La Luna Formation. Our goals are to reconstruct the lower Umir Formation paleoenvironmental setting and assess the possible occurrence of a basal unconformity with the La Luna Formation.

Institutional abbreviations

UNISINOS, Universidade do Vale do Rio dos Sinos, São Leopoldo, Brasil; **itt OCEANEON,** Instituto Tecnológico de Paleoceanografia e Mudanças Climáticas, São Leopoldo, Brasil; **UIS,** Universidad Industrial de Santander, Bucaramanga, Colombia.

MATERIAL AND METHODS

Studied section

We sampled sediments from the Aguablanca Creek section in the Middle Magdalena Basin (7°7’ N, 73°18’ W; Eastern Colombian Cordillera). This locality was previously studied by Terraza (2019), and we focused on the uppermost interval investigated by

this author (320.8-344.2 m stratigraphic height), which comprises the uppermost part of the La Luna Formation (La Renta Formation *sensu* Terraza, 2019) and the lower segment of Umir Formation (Figs. 1-3). The La Luna Formation is composed mainly of homogeneous limestones (mainly packstones) and a ~25 cm thick greenish glauconitic sandstone at its top. The Umir Formation is composed of a monotonous succession of dark grey marlstones, mudstones, and siltstones. The La Luna-Umir contact was proposed at 322.8 m by Terraza (2019).

Methods

Micropaleontological samples (n=28; interval 320.8-344.2 m stratigraphic height) were prepared according to standard methods at itt OCEANEON (UNISINOS). Approximately 30 g of dried rock were soaked into a 5% hydrogen peroxide (H_2O_2) solution for about 36 hours, washed over 63 and 150 µm sieves, and dried at 40°C (Sohn, 1961). Due to moderate and poor abundance, respectively, all foraminifers and ostracods were handpicked. Planktonic foraminiferal taxonomy followed Caron (1985), Nederbragt (1991), Georgescu (2005), Premoli Silva and Verga (2011), among others. Benthic foraminiferal taxonomy followed previous studies of Maastrichtian units in Colombia (Cushman and Hedberg, 1930, 1941; Martínez, 1989; Tchegliakova 1993, 1995; Tchegliakova and Mojica, 2001; Patarroyo et al., 2017, 2022), and regional literature for the tropics and the US Western Interior (Sellier de Civrieux, 1952; Frizzell, 1954; Bolli et al., 1994). Ostracod suprageneric classification follows Scott (1961). Selected foraminiferal specimens were imaged using an EVO MA15 Zeiss scanning electron microscope (SEM), and all studied specimens are archived in the micropaleontological collections at itt OCEANEON. Total microfossil counts and their diversity estimations are given in Supplementary Table S1.

Nannofossil samples (n=27; interval 321.2-344.2 m) were also prepared at itt OCEANEON following the smear-slide technique detailed by Bown and Young (1998), and studied using a Zeiss Axio Imager A2 petrographic microscope, at 1000x magnification. In order to achieve a quantitative analysis of the assemblages, 700 fields of view (FOV) were counted per slide. Preservation of calcareous nannofossils was evaluated under a light microscope using qualitative criteria: “Good” indicating specimens with little or no etching and/or overgrowth; “moderate” for specimens exhibiting some degree of etching and/or overgrowth, but still easily recognizable; and “poor” for specimens exhibiting extreme etching and/or overgrowth (Roth, 1983). Total calcareous nannofossil counts are given in Supplementary Table S2.

Diversity (Shannon-H), richness (S) and evenness (E) estimations were calculated using the software Past version 2.15 (Hammer et al., 2001), in addition to an SHEBI (“SHE Analysis for Biozone Identification”) analysis, which is defined by the natural logarithm (ln) of the evenness estimations. SHEBI analysis searched general trends in ln(E) values in order to identify different assemblage intervals in the section (Buzas and Hayek, 1998, 2005).

A geochemical survey was conducted with bulk sediment samples from the section. Sample aliquots of 5 to 10 g ground rock (n = 29; interval 320.8-344.2 m height) were measured with a PanAlytical Epsilon 1 X-ray fluorescence (XRF) spectrometer at itt OCEANEON, with elemental concentrations reported as raw counts per second (cps). Results were normalized to a median-scaled (NMS) following Lyle et al. (2012) and interpreted as simple and logarithmic elemental ratios. We used the log(Fe/Ca) ratio as a proxy for terrigenous sediments input versus carbonate production (*e.g.* Govin et al., 2012), and the Sr/Ba ratio as a salinity proxy (*e.g.* Wei and Algeo, 2019). Bottom water oxygenation was evaluated with the NMS intensities of redox-sensitive trace metals

(TM) Ni, Cu, V, and Zn normalized by NMS Al intensities (*e.g.* Dummann et al., 2021). XRF measurements are provided in Supplementary Table S3.

RESULTS

Microfossil occurrences

The micropaleontological record of the Aguablanca Creek section yielded heterogeneous assemblages. Foraminiferal assemblages of the La Luna Formation and of the glauconitic level at the contact with the Umir Formation yielded few specimens of *Lenticulina* spp., undetermined rotaliids and planktonic foraminifera. Abundance and diversity increased along the succession of the Umir Formation (Figs. 2, 3), where at least two intervals can be recognized based on the composition of foraminiferal assemblages: (1) a lower interval (329-338.2 m stratigraphic height) mainly composed of benthic taxa such as *Haplophragmoides excavatum*, *Gavelinella* spp., *Gyroidinoides depressus*, *Lenticulina muensteri*, *Orthokarstenia cretacea*, *Praebulimina* spp., *Pyramidina triangularis*, and *Siphogenerinoides bramletti*, while the planktonic assemblages were mainly composed of biserial taxa (*Planoheterohelix* spp., *Pseudoguembelina* spp., *Spiroplecta americana*) and scarce trochospiral forms such as *Archaeoglobigerina* spp., *Rugoglobigerina* spp., *Muricohedbergella* spp., and *Globotruncana aegyptiaca* (Fig. 3); and (2) an upper interval (340-344.2 m) mainly dominated by undetermined textulariids and few specimens of *Ammobaculites colombiana* (sample 343 m; Figs. 2, 3).

Nannofossil assemblages, in contrast, were equally abundant in the La Luna and Umir formations, though species such as *Cervisella operculata*, *Cribrosphaerella ehrenbergii*, *Micula staurophora*, or *Reinhardtites levis* were more common in the La Luna Formation (Figs. 4,5). *Chiastozygus synquadriperforatus*, *Cylindralithus biarcus*,

Cylindralithus serratus, and *Predicosphaera stoveri* were only present in the Umir Formation, but with low abundances. The interval 340-344.2 m was barren of calcareous nannofossils, though samples at 340 m and 340.5 m yielded abundant (>300 fragments/sample) ascidian spicules (Fig. 4).

Other microfossils recovered from the Aguablanca Creek section include fish teeth, gastropod fragments, and ostracods (Fig. 2). Poor preservation and the scarcity of ostracods hampered taxonomic descriptions, and only a single specimen of *Actinocythereis*? sp. at 337.6 m was identified.

Diversity (Shannon-H), evenness (E), and richness (S) estimations for foraminiferal and the calcareous nannofossil assemblages varied throughout the section. In the interval with better foraminiferal recovery (329.9-338.2 m), richness was relatively high (S>10), while the Shannon-H index was >2 for most samples (Figure 6). Calcareous nannofossil richness was also higher in this interval (S>10), and some other specific levels in the Umir Formation such as 331 and 331.3 m (reaching S>35). Regarding calcareous nannofossil diversity, the Shannon-H index ranged from 1.2 to 2.0, with the highest values (H>2) at 322.5 m and 335.5. m, while the smallest value (H<1.1) was recorded in the lower part of the section (321.2-321.6 m). Evenness estimations in the calcareous nannofossil assemblages also presented a wide range of values along the section (0.1 to 0.7), though samples of the Umir Formation presented mostly values around 0.6 in the upper part of the section. Finally, SHEBI analysis, based on ln(E) values of calcareous nannofossil assemblages, suggests the occurrence of at least two assemblage intervals: (1) a lower assemblage (321.2-331.3 m) with most of the samples having values of ln(E)>-1.2, and (2) an upper assemblage, comprising samples of the Umir Formation (333.9-339 m) with values of ln(E)<-1.0 (Fig. 6).

Geochemical proxies

Log(Fe/Ca) presents an upward-increasing trend at the Aguablanca Creek section, with values ranging between –0.1 and 1.8. Conversely, the Sr/Ba ratio presents a decreasing-upward trend, with values ranging from 130 to 90 in the lower part of the section and values <30 for most of the samples of the Umir Formation (Fig. 6). Most of the trace metals (TM)/Al ratios exhibit similar trends throughout the section, presenting a steady decrease above the contact between the La Luna and Umir formations. For instance, the Ni/Al, Cu/Al, and Zn/Al ratios present higher values in the La Luna Formation (5-$10*10^{-7}$ in the Ni/Al and Cu/Al, $>38*10^{-7}$ in the Zn/Al) and drop to average values of $4*10^{-7}$ and $25*10^{-7}$, respectively, within the Umir Formation. The V/Al ratio presents relatively high values in the La Luna Formation (19-$26*10^{-7}$), drops abruptly at the contact between the two formations, and shows an upward-increasing trend across the Umir Formation (Fig. 6).

DISCUSSION

Biostratigraphic constraints for Maastrichtian strata at the Aguablanca Creek section

Micropaleontological evidence supports a latest Cretaceous (Campanian-Maastrichtian) age for the studied interval in the Aguablanca Creek section (Figs. 2, 4, 7). Most of the recovered planktonic foraminiferal taxa have wide chronostratigraphic ranges (*Planoheterohelix globulosa*, *Muricohedbergella* spp.), but there are some species such as *Spiroplecta americana*, *Pseudoguembelina excolata*, *Rugoglobigerina macrocephala* and *Globotruncana aegyptiaca* with late Campanian-late Maastrichtian ranges. Benthic foraminiferal assemblages of the Umir Formation can be assigned to the *Siphogenerinoides bramletti* (329.9-337.6 m) and *Ammobaculites colombiana* (338.2-344.2 m) assemblage zones, according to the definitions of Cushman and Hedberg

(1941) in the more proximal Catatumbo basin. Following these authors, as well as the chronostratigraphic update of Martinez (1989) based on planktonic foraminifera and new micropaleontological data for the Cesar-Ranchería and Catatumbo basins (Patarroyo et al., 2017; 2022), the *S. bramletti* and *A. colombiana* assemblage zones comprise the late Maastrichtian (*Abathomphalus mayaroensis* Zone to probably *Plummerita hantkeninoides* Zone). In general, foraminiferal assemblages from the Aguablanca Creek section present the same sequence of biostratigraphic markers reported by Martinez (1989) and Patarroyo et al. (2017, 2022) for the coetaneous Colón Formation, located in the Catatumbo and Cesar-Ranchería basins (Fig. 7). The absence of diagnostic foraminifers in the upper part of the La Luna Formation hampered an age assignment for this unit.

The Umir Formation was originally dated as a Campanian-Maastrichtian by Petters (1955), using benthic foraminiferal assemblages that were also recognized in Western Venezuela. That scheme used the same biozones as Cushman and Hedberg (1941), with a difference in the definition of the oldest biozone (*Orthokarstenia cretacea* instead of *Pullenia cretacea*). A key aspect in the biostratigrahic zonation of Petters (1955) was the calibration with ammonite markers. For instance, in the southern MMV, the Campanian ammonite *Stantonoceras* occurred within the *O. cretacea* zone. Ammonite genera such as *Coahuilites* and *Sphenodiscus* within the *S. bramlettei* and *A. colombiana* foraminiferal zones confirmed a Maastrichtian age for the upper part of the Umir Formation. However, the precise location and detailed description of that material remained unclear, hampering more detailed comparisons (*e.g.* Ward et al., 1973). Later, a series of studies by Tchegliakova (1993, 1995, 1996) in the La Julia Creek section (northeastern MMV) and the Honda-Guaduas area (southern MMV) discussed the Campanian age assignment for the lower segment of the Umir Formation. At the La

Julia Creek section, where the La Luna-Umir formations contact occurs, Tchegliakova (1995) reported the occurrences of *A. colombiana* and the planktonic species *Rugoglobigerina macrocephala*, constraining the age of the Umir Formation to middle-late Maastrichtian, and probably an early Maastrichtian age for the upper part of the La Luna Formation. Moreover, in localities from the Honda-Guaduas area, Tchegliakova (1996) identified the planktonic foraminiferal biozones *Gansserina gansseri* and *Abathomphalus mayaroensis*, extending the chronostratigraphic range of the lower Umir Formation from the middle Maastrichtian to the uppermost Campanian (Fig. 7). Considering our interpretation of a Maastrichtian age for the Umir Formation, based exclusively on the record of the foraminiferal assemblages, the absence of diagnostic elements of the *O. cretacea* assemblage zone (e.g. *Pullenia cretacea*) in the studied material, and the location of the Aguablanca Creek section (middle part of the MMV), it is plausible that the lower boundary of the formation is diachronous along the MMV. However, it must be also considered that the lowermost segment of the Umir Formation is covered in the Aguablanca Creek section (324.1-329.9 m).

Considering these uncertainties, one of our goals was to explore an integrated approach (calcareous nannofossils, ostracods) in order to get higher accuracy for the age span of the studied section. Studies on calcareous nannofossils from the Late Cretaceous successions of Colombia are scarce, being Pérez-Panera et al. (2018) the only published work. That study focused mainly on the La Luna Formation and the lowermost part of the Umir Formation from an exploratory well in the northernmost MMV, and reported most of the species we recovered at the Aguablanca Creek section. Calcareous nannofossil assemblages in our locality were mainly composed of taxa with long chronostratigraphic ranges (*e.g.* Aptian-Maastrichtian). However, species such as *Arkhangelskiella cymbiformis*, *Ceratolithoides aculeus*, *Perchnielsenella stradneri* and

307 *Prediscosphaera stoveri*, which ranged from Campanian to Maastrichtian, were present
308 in low abundances along the section. The last occurrence of *Reinhardtites levis* at 331 m
309 could be used as a boundary between the early and late Maastrichtian (top of UC18
310 zone), though its rare occurrence, and the presence of benthic foraminifer *S. bramletti* in
311 this interval, could be interpreted as a product of reworking. Using the calcareous
312 nannofossil record, an age not older than early Maastrichtian could be assigned to the
313 lowermost part of the Umir Formation (324.1-331 m).
314 Though calcareous nannofossil assemblages in the La Luna Formation were more
315 abundant and diversified than foraminiferal assemblages, and the SHEBI analysis
316 suggests a floristic turnover, taxa of the La Luna Formation consist of species with long
317 chronostratigraphic ranges and Campanian-Maastrichtian markers. Therefore, based on
318 the calcareous nannofossils assemblages we suggest a Campanian to early Maastrichtian
319 age for the top of the La Luna Formation (Fig. 7). Our interpretation slightly modifies
320 the original conclusions of Terraza (2019), who assigned a Campanian age to the upper
321 part of the La Luna Formation (=La Renta Formation) in the Aguablanca Creek section.
322 That age assignment was based on the presence of Santonian ammonites such as
323 *Plesiotexanites*, *Texanites* and *Cocuyites* in underlaying strata of the section (middle
324 part of the La Luna Formation; Galembo Formation *sensu* Terraza, 2019), and the
325 common presence of the benthic foraminifer *O. cretacea* in thin sections from the upper
326 part of the La Luna Formation (=Galembo Formation). Additionally, the lithological
327 contrast between the La Luna and Umir formations suggests the presence of an
328 unconformity according to that author. The paleoenvironmental nature of the La Luna-
329 Umir contact will be discussed in the following section.
330 Our biostratigraphic interpretation for the uppermost part of the Aguablanca Creek
331 section (340-344.2 m) is tentative, considering the absence of calcareous nannofossils

above 339 m, and the presence of scarce ostracods and benthic foraminifers, the latter represented mostly by agglutinated taxa. So far, we can only assign an age not older than late Maastrichtian, based on the first occurrence of the benthic foraminiferal species *A. colombiana* at 343 m, which defines the base of its homonym assemblage zone (Cushman and Hedberg, 1941). New micropaleontological data in the Cesar-Rancheria Basin and the identification of the Cretaceous-Paleogene (K-Pg) boundary in that area have provided a better age control for the *A. colombiana* assemblage zone (De La Parra et al., 2022; Patarroyo et al., 2022).

Considering the expected abundance decrease of marine microfossils in the uppermost strata at our section, palynological analyses could improve the chronostratigraphy of the middle and upper parts of the Umir Formation. Maastrichtian strata from the Umir Formation were originally studied by Van der Hammen (1954, 1957), who proposed three palynological zones (Maastrichtian A-C). However, since most of the morphotypes described by Van der Hammen (1954, 1957) have been revised and assigned to other genera, new biostratigraphic schemes have been proposed since then for Maastrichtian strata in Colombia (Sarmiento, 1992; Yepes, 2001; Santos, 2012; De La Parra et al., 2022).

Paleoenvironmental settings recorded at the Aguablanca Creek section

The stratigraphic description of Terraza (2019), as well as the micropaleontological and geochemical data from our study at Aguablanca Creek section, highlight the differences between the La Luna Formation and the Umir Formation. Contrasting sedimentological and stratigraphical characteristics have been traditionally interpreted as evidence of a regional unconformity, related to the first pulses of the Andean orogeny (*e.g.* Ward et al., 1973; Sarmiento et al., 2015). However, the nature of this boundary and its presence in other basins have been intensively debated in recent years. Based on

sedimentological studies in the Cocuy region, Bayona et al. (2020) defined it as a xenoconformity, considering that it reflects a shift in the depositional regime (from dominant carbonate deposition to the onset of synorogenic terrigenous-dominated deposition), instead of a major hiatus within the Maastrichtian sedimentary successions. Petrographic, paleontological (microfossils), geochemical (total organic carbon, TOC), and seismic data also evidence marked differences between the La Luna Formation and the Colón Formation (coeval to the Umir Formation) in the Catatumbo and Cesar-Ranchería basins (Ayala-Calvo et al., 2009; Cooney and Lorente, 2009; Bayona et al., 2011; Patarroyo et al., 2017).

The dominance of carbonate rocks and the presence of calcareous nannofossils in the Aguablanca Creek section suggest open marine conditions, probably in a middle shelf setting, for the upper part of the La Luna Formation (Fig. 7). This is also supported by our geochemical results, since sediment Sr/Ba values of the uppermost La Luna Formation indicate higher paleosalinity in comparison with the overlying strata. Strontium tends to be absorbed on fine-grained sediments deposited under high-salinity waters, whereas barium content is higher in freshwater delivered by continental runoff (Wei and Algeo, 2019). Additionally, increased concentrations of redox-sensitive TM, such as V, Ni, Cu and Zn, suggest that sediments were deposited under the influence of oxygen-depleted bottom waters (Fig. 6; *e.g.* Dummann et al., 2021). Previous studies in the upper part of the La Luna Formation in the MMV and other basins have reported an overall high total organic carbon (TOC) content, with values ranging from 3 to 7 % (Patarroyo et al., 2021). The low abundance of benthic foraminifers in this part of the section could be, in fact, a consequence of poorly oxygenated bottom waters. However, taphonomic controls are not discarded as a possible cause of low foraminiferal abundances, since some of the analyzed samples were collected from the greenish

glauconitic sandstone below the La Luna-Umir contact. Special caution must additionally be taken for interpreting this interval, since reworked intraclasts were reported by Terraza (2019) and by studies in other localities recording the same glauconitic level in the MMV (*e.g.* Ward et al., 1973; Sarmiento et al., 2015). In fact, glauconite precipitation supports our paleoenvironmental interpretation for the La Luna Formation, since glauconite has been reported from shallow marine poorly oxygenated settings in the Maracaibo area (*e.g.* Erlich et al., 1999; Parra et al., 2003).

In contrast to the La Luna Formation, the microfossil content and geochemical proxies (Sr/Ba and log(Fe/Ca) ratios) of the uppermost part of our section indicate a progressive transition from an inner platform to sublittoral settings within the Umir Formation (Fig. 6).

Foraminiferal distributions depict two intervals that illustrate this transition: a lower assemblage (329-338.2 m) dominated by calcareous benthic foraminifers (mostly elongated and planispiral forms) and some planktonic taxa (mostly biserial forms); and an upper assemblage (340-344.2 m), characterized by lower recovery, but dominated by agglutinated benthic taxa, which tend to increase in abundance at relatively shallow conditions (Figs. 2, 7; *e.g.* Cetean et al., 2011). Like in other studies on latest Cretaceous foraminifera from Colombia, the disappearance of keeled planktonic taxa (only present in the interval 334.9-336 m), the predominance of the benthic foraminifera, and the increase in the proportion of textulariids upward in the succession, suggest a regressive pattern for this unit (Bürgl and Dummit, 1954; Martínez, 1989; 2003; Vergara, 1997; Guerrero et al., 2000; Tchegliakova and Mojica, 2001; Patarroyo et al., 2022). This regressive stacking trend was previously documented with foraminiferal assemblages within the Umir Formation, but without a broad stratigraphic control (Petters, 1955; Tchegliakova 1993, 1995). In the La Julia Creek section,

Tchegliakova (1993, 1995) reported assemblages mostly composed of agglutinated forms (*Haplophragmoides*, *Bathysiphon*, *A. colombiana*), unidentified ostracods, calcareous algae, and high proportions of amorphous organic matter, suggesting paralic environments with intermittent influence of freshwater input.

Other micropaleontological evidence of this shallowing-upward trend include the disappearance of the calcareous nannofossil above 339 m, as well as the abundance of ascidian spicules (>300 specimens/sample) at 340 m and 340.5 m at the Aguablanca Creek section (Fig. 4). Considering that some species are temperature and salinity-sensitive (Shenkar and Swalla, 2011), future studies on these microfossils of the Umir Formation could provide new insights into its paleoenvironmental evolution.

Proxy records at the Aguablanca Creek section also provided clues about the shallowing trend recorded by the Umir Formation (Fig. 6). For instance, fluctuations in the log(Fe/Ca) ratio can be used as a tracer of terrigenous input relative to carbonate sedimentation (Govin et al., 2012). The log(Fe/Ca) at the Aguablanca Creek section indicates a steady increase upward in the section, in comparison with the lower values within the La Luna Formation, implying increased supply of terrigenous sediments likely associated with progressively more proximal settings. Relatively lower sediment Sr/Ba values at the uppermost Aguablanca Creek section also suggest increased freshwater input (Wei and Algeo, 2019), which is consistent with more proximal depositional settings.

At a regional scale, Maastrichtian sea-level fluctuations within the Umir Formation include at least five maximum flooding surfaces over a major retro-gradational sequence (Montaño et al., 2016). However, that study was mostly focused on the middle to upper interval of the unit, which yields economically relevant coal-bearing strata. The geological evolution of Maastrichtian coastal environments in northern South America

was highly dynamic and was not solely affected by sea level fluctuations, but also deeply influenced by the onset of tectonic activity in the Central and Eastern Cordilleras during the Campanian-Maastrichtian (Fig. 7; Villamil and Pindell, 1998; Sarmiento-Rojas, 2019; Montes et al., 2019; Bayona et al., 2020).

Finally, our micropaleontological and geochemical results suggest moderate oxygenation of bottom waters for the lower part of the Umir Formation. In general, there is a high proportion of benthic infaunal taxa along the Aguablanca Creek section, comprising elongated (*e.g. Siphogenerinoides*, *Orthokarstenia*, *Stilostomella*), ovoidal (buliminids) and elongated biserial (*e.g. Coryphostoma*, *Loxostomum*) forms. These morphotypes are usually interpreted as indicative of poorly oxygenated bottom water conditions, related to water mass eutrophication (Van der Akker et al., 2000; Jorissen et al., 2007). However, there were still moderate abundance and richness of epifaunal or shallow infaunal taxa (*e.g. Gavelinella*, *Gyroidinoides*, *Lenticulina*) within this interval at the Aguablanca Creek section. Overall, benthic foraminiferal assemblages at the Aguablanca Creek section contrast with those described for the La Luna Formation and coeval units in Colombia, which recorded relatively high primary productivity, recurrent anoxic episodes, and yielded benthic foraminiferal assemblages dominated by deep infaunal forms (*e.g.* buliminids; Vergara, 1997; Guerrero et al., 2000; Tchegliakova and Mojica, 2001; Martinez, 2003; Parra et al., 2003; Patarroyo et al., 2017).

Values of TM/Al ratios within the Umir Formation are low in comparison to those of the La Luna Formation (Fig. 6), suggesting improved bottom water oxygenation (*e.g.* Dummann et al., 2021). Nevertheless, fine-grained sediments of the lower part of the Umir Formation show TOC contents below 1.7 %, while the organic carbon-rich levels from the middle and upper part of this unit have TOC values ranging from 12 to 40%

(Rangel et al., 2000). An exception among the overall trends of TM/Al proxies at the Aguablanca Creek section is the V/Al ratio, which depicts a trend similar to that of the log(Fe/Ca) ratio, and in contrast to the remaining TM (Fig. 6). One likely explanation for the V/Al trend would be the input of V-rich terrigenous sediments.

CONCLUSIONS

The integrated micropaleontological (foraminifers, calcareous nannofossils, and ostracods) and geochemical (log(Fe/Ca), Sr/Ba, and redox-sensitive TM/Al ratios) study of the Maastrichtian stratigraphic succession at Aguablanca Creek section revealed a major paleoenvironmental shift between the La Luna and Umir formations. Based on the common presence of calcareous nannofossils and higher concentrations of redox-sensitive trace metals such as Ni, Cu, and Zn, we interpret the upper part of the La Luna Formation as a middle shelf setting, with poorly oxygenated bottom water conditions. In contrast, benthic foraminiferal, log(Fe/Ca), and Sr/Ba records depict a shallowing-upward trend for the studied interval of the Umir Formation in a retro-gradational inner platform setting. This interval is characterized by a gradual decrease of the planktonic biota (heterohelicids, keeled foraminifers, calcareous nannofossils), and the transition from moderately diverse calcareous benthic foraminifers (buliminids, elongated uniserial, trochospiral forms) to poorly diversified assemblages, composed of agglutinated benthic forms (*Ammobaculites*, unidentified textulariids). This interpretation is also supported by bulk sediment Sr/Ba and log(Fe/Ca) ratios, which indicate increased continental runoff and terrigenous input in the upper part of the section, likely associated with more proximal depositional settings. The recorded paleoenvironmental turnover suggests the presence of a xenoconformity at the La Luna-Umir stratigraphic contact. Our biostratigraphic results suggest an early Maastrichtian

age (base of the regional foraminiferal zone *Siphogenerinoides bramletti*) for this unconformity.

ACKNOWLEDGMENTS

The authors thank the staff of itt-OCEANEON for their support with sample preparation and analyses. G.D.P. thanks PETROBRAS for a scholarship in the project "Bioestratigrafia de foraminíferos do Aptiano-Albiano da Margem Continental Brasileira". L.A. acknowledges funding from project PID2019-105537RB-I00 funded by MCIN/AEI/ 10.13039/501100011033 and by "ERDF A way of making Europe". Gustavo Torres (Stratos Consultoría Geológica, Colombia) kindly assisted with edition of foraminiferal SEM images. Andrea Caramés (UBA) and an anonymous reviewer provided key suggestions in order to improve the first version of this contribution, and to them we express our gratitude.

REFERENCES

Ayala-Calvo, R.C., Bayona-Chaparro, G.A., Ojeda-Marulanda, C., Cardona, A., Valencia, V., Padrón, C.E., Yoris, F., Mesa-Salamanca, J., & García, A. (2009) Estratigrafía y procedencia de las unidades comprendidas entre el Campaniano y el Paleógeno en la subcuenca de Cesar: aportes a la evolución tectónica del área. *Geología Colombiana,* 34, 3–33.

Bayona, G., Baquero, M., Ramírez, C., Tabares, M., Salazar, A.M., Nova, G., Duarte, E., Pardo, A., Plata, A., Jaramillo, C., Rodríguez, G., Caballero, V., Cardona, A., Montes, C. Gómez-Marulanda, S., & Cárdenas-Rozo, A.L. (2020) Unravelling the widening of the earliest Andean northern orogen: Maastrichtian to early

506 Eocene intra-basinal deformation in the northern Eastern Cordillera of
507 Colombia. *Basin Research,* 33, 809–845.
508 Bayona, G., Montes, C., Cardona, A., Jaramillo, C., Ojeda, G., & Valencia, V. (2011)
509 Intraplate subsidence and basin filling adjacent to an oceanic arc-continental
510 collision: a case from the southern Caribbean–South America plate margin.
511 *Basin Research,* 23. http://dx.doi.org/10.1111/j.1365-2117.2010.00495.x.
512 Bolli, H.M., Beckmann, J.P., & Saunders, J.B. (1994) *Benthic foraminiferal*
513 *biostratigraphy of the South Caribbean region*. Cambridge University Press.
514 Cambridge.
515 Bown, P.R., & Young, J.R. (1988) Techniques. In: Bown, P.R. (Ed.). *Calcareous*
516 *Nannofossil Biostratigraphy* (pp. 16–28). British Micropaleontological Society
517 Series.
518 Bürgl, H., & Dumit, Y. (1954) El Cretáceo Superior en la región de Girardot. *Boletín*
519 *Geológico,* 2, 23–48.
520 Buzas, M.A., & Hayek L.A.C. (1998) SHE analysis for biofacies identification
521 *Journal of Foraminiferal Research*, 28, 233–239.
522 Buzas, M.A., & Hayek L.A.C. (2005) On richness and evenness within and between
523 communities. *Paleobiology,* 31, 199–220.
524 Caron, M. (1985) Cretaceous planktic foraminifera. In H. M. Bolli, J. Saunders, & K.
525 Perch-Nielsen (Eds.). *Plankton Stratigraphy* (pp. 17–86). Cambridge.
526 Carvalho, M.R., Jaramillo, C., De La Parra, F., Caballero-Rodríguez, D., Herrera, F.,
527 Wing, S., Turner, B.L., D'Apolito, C., Romero-Báez, M., Narváez, P., Martínez,
528 C., Gutierrez, M., Labandeira, C., Bayona, G., Rueda, M., Paez-Reyes, M.,
529 Cárdenas, D., Duque, A., Crowley, J.L., Santos, C., & Silvestro, D. (2021)

Extinction at the end-Cretaceous and the origin of modern Neotropical rainforests. *Science*, 372, 63–68.

Cetean, C.G., Bălc, R., Kaminski, M.A., & Filipescu, S. (2011) Integrated biostratigraphy and palaeoenvironments of an upper Santonian – upper Campanian succession from the southern part of the Eastern Carpathians, Romania. *Cretaceous Research*, 32(5), 575–590.

Cooney, P.M., & Lorente, M.A. (2009) A structuring event of Campanian age in western Venezuela, interpreted from seismic and paleontological data. *Geological Society Special Publications*, 328, 687–703.

Cushman, J.A., & Hedberg, H.D. (1930) Notes on some foraminifera from Venezuela and Colombia. *Contributions from the Cushman Laboratory for Foraminiferal Research*, 6, 64–69.

Cushman, J.A., & Hedberg, H.D. (1941) Upper Cretaceous foraminifera from Santander del Norte, Colombia. *Contributions from the Cushman Laboratory for Journa of the Foraminiferal Research*, 17, 79–100.

De La Parra, F., Jaramillo, C., Kaskes, P., Goderis, S., Claeys, P., Villasante-Marcos, V., Bayona, G., Hatsukawa, Y., & Caballero, D. (2022) Unraveling the record of a tropical continental Cretaceous-Paleogene boundary in northern Colombia, South America. *Journal of South American Earth Sciences*, 114, 103717.

Dummann, W., Hofmann, P., Herrle, J.O., Wennrich, V., & Wagner, T. (2021) A refined model of Early Cretaceous South Atlantic–Southern Ocean gateway evolution based on high-resolution data from DSDP Site 511 (Falkland Plateau). *Palaeogeography, Palaeoclimatology, Palaeoecology*, 562, 110113.

Erlich, R.N., Macsotay, O., Nederbragt, A.J., & Lorente, M.A. (1999) Palaeoecology, palaeogeography and depositional environments of Upper Cretaceous rocks of

western Venezuela. *Palaeogeography, Palaeoclimatology, Palaeoecology*, 153(1–4), 203–238.

Frizzell, D.L. (1954) *Handbook of Cretaceous Foraminifera of Texas*. University of Texas at Austin, Bureau of Economic Geology Report of Investigations, 22, 1–237.

Garzón, S., Warny, S., & Bart, P.J. (2012) A palynological and sequence-stratigraphic study of Santonian–Maastrichtian strata from the Upper Magdalena Valley basin in central Colombia. *Palynology*, 36, 112–133.

Georgescu, M.D. (2005) On the systematics of rugoglobigerinids (planktonic foraminifera, Late Cretaceous). *Studia Geologica Polonica*, 124, 87–97.

Govin, A., Holzwarth, U., Heslop, D., Ford Keeling, L., Zabel, M., Mulitza, S., Collins, J.A., & Chiessi, C.M. (2012) Distribution of major elements in Atlantic surface sediments (36°N–49°S): Imprint of terrigenous input and continental weathering. Geochem. *Geophys. Geosyst*. 13. DOI:10.1029/2011gc003785.

Gramal-Aguilar, A., Carranco-Andino, F., Romero-Cóndor, C., Pulupa-Vela, R., Calderón-Romero, D., & Toainga-Oñate, S. (2021) Evidencias de canibalización de secuencias Cretácicas y Paleógenas de la Cuenca Oriente en la cuña orogénica de los Andes ecuatorianos. *Boletín de Geología,* 43(3), 15–34.

Guerrero, J., Sarmiento, G., & Navarrete, R.E. (2000) The Stratigraphy of the W side of the Cretaceous Colombian basin in the Upper Magdalena Valley. Reevaluation of selected areas and type localities including Aipe, Guaduas, Ortega, and Piedras. *Geología Colombiana*, 25, 45–110.

Hammer, O., Harper, D.A.T., & Ryan, P.D. (2001) PAST: paleontological statistics software package for education and data analysis. *Palaeontologia Electronica,* 4(1), 1–9.

580 Hardenbol, J., Thierry, J., Farley, M., Jacquin, T., De Graciansky, P., & Vail, P. (1998)
581 Mesozoic and Cenozoic sequence chronostratigraphic framework of European
582 basins. In P. Graciansky, J. Hardenbol, T. Jacquin, P. Vail, & M. Farley (Eds.)
583 *Mesozoic and Cenozoic Sequences Stratigraphy of European Basins* (pp. 3–13).
584 SEPM Special Publication 60.
585 Huber, B.T., MacLeod, K.G., Watkins, D.K., & Coffind, M.L. (2018) The rise and fall
586 of the Cretaceous Hot Greenhouse climate. *Global and Planetary Change*, 167,
587 1–23.
588 Jorissen, F.J., Fontanier, C., & Thomas, E. (2007) Paleoceanographical indicators based
589 on deep-sea benthic foraminiferal assemblage characteristics. *Developments in*
590 *Marine Geology*, 1, 263–325.
591 Kominz, M.A., Browning, J.V., Miller, K.G., Sugarman, P.J., Mizintsevaw, S. &
592 Scotese, C.R. (2008) Late Cretaceous to Miocene sea-level estimates from the
593 New Jersey and Delaware coastal plain coreholes: an error analysis. *Basin*
594 *Research*, 20, 211–226.
595 Lyle, M., Olivarez-Lyle, A., Gorgas, T., Holbourn, A., Westerhold, T., Hathorne, E. C.,
596 Kimoto, K., & Yamamoto, S. (2012) Data report: raw and normalized elemental
597 data along the U1338 splice from X-ray Fluorescence scanning. *Proceedings of*
598 *the Integrated Ocean Drilling Program*, 320/321,
599 DOI:10.2204/iodp.proc.320321.2010
600 Martínez, R. J.I. (1989) Foraminiferal biostratigraphy and paleoenvironments of the
601 Maastrichtian Colón mudstones of Northern South America. *Micropaleontology*,
602 35(2), 97–113.
603 Martínez, J.I. (2003) The Paleoecology of late Cretaceous upwelling events from the
604 Upper Magdalena Basin, Colombia. *Palaios*, 18(4–5), 305–320.

605 Martinez, J.I., & Hernandez, R. (1992) Evolution and drowning of the Late Cretaceous
606 Venezuelan carbonate platform. *Journal of South American Earth Sciences*,
607 5(2), 197–210.
608 Montaño, P.C., Nova, G., Bayona, G., Mahecha, H., Ayala, C., Jaramillo, C., & De La
609 Parra, F. (2016) Análisis de secuencias y procedencia en sucesiones
610 sedimentarias de grano fino: un ejemplo de la Formación Umir y base de la
611 Formación Lisama, en el sector de Simacota (Santander, Colombia). *Boletín de*
612 *Geología*, 38(1), 51–72.
613 Montes, C., Rodríguez-Corcho, A.F., Bayona, G., Hoyos, N., Zapata, S., & Cardona, A.
614 (2019) Continental margin response to the multiple arc-continent collisions: The
615 northern Andes-Caribbean margin. *Earth Science Reviews*, 198, 102903.
616 Navarrete, R.E., Parra, F.J., Pérez-Panera, J.P., Daza, D., Sánchez, C., Prince, M., &
617 Rodríguez, M. (2018) Turonian-Campanian foraminifera zonation for the La
618 Luna and lower Umir formations, Middle Magdalena Valley Basin, northern
619 Colombia. In Cusminsky et al. (Eds.) *Advances in South American*
620 *Micropaleontology - Selected papers of the 11th Argentine Paleontological*
621 *Congress* (pp. 67–114). Springer Earth System Science Series.
622 Nederbragt, A. (1991) Late Cretaceous biostratigraphy and development of
623 Heterohelicidae (planktic foraminifera). *Micropaleontology*, 37(4), 329–372.
624 Parra, M., Moscardelli, L., & Lorente, M.A. (2003) Late Cretaceous anoxia and lateral
625 microfacies changes in the Tres Esquinas Member, La Luna Formation, Western
626 Venezuela. *Palaios*, 18, 321–333.
627 Patarroyo, G.D, Alarcón, C.M., Torres, J.M., Díaz, J.S., Gómez, J.S., Márquez, J.J.,
628 Pontón, L.A., & Barragán, D.M. (2021) Reconocimiento geológico de la

Formación La Luna en el sector de Matanza (Oeste del Macizo de Santander, Colombia). *Boletín de Geología*, 43(1), 35–51.

Patarroyo, G.D., Kochhann, K.G.D., Ceolin, D., Guerra, R., Alegret, L., & Bom, M.H.H. (2022) Paleoenvironmental changes recorded at a late Maastrichtian marine succession of Northern South America. *Journal of South American Earth Sciences*, 119, 104015.

Patarroyo, G.D., Torres, G.A., Rincón, D.A., Cárdenas, C.P., & Márquez, R.E. (2017) Bioestratigrafía e inferencias paleoambientales de las asociaciones de foraminíferos en las formaciones cretácicas La Luna-Colón (Cuenca del Catatumbo, Colombia). *Boletín de Geología*, 39(3), 25–40.

Pérez-Panera, J.P., Parra, F.J., Navarrete, R.E., Sánchez, C., Daza, D., Rodriguez, M., & Prince, M. (2018) Turonian–Santonian Calcareous Nannofossil Biozonation for La Luna Formation, Middle Magdalena Valley Basin, Northern Colombia. In Cusminski et al. (Eds.) *Advances in South American Micropaleontology-Selected papers of the 11th Argentine Paleontological Congress*. Springer Earth System Science Series, pp. 46–66.

Petters, V. (1955) Development of Upper Cretaceous foraminiferal faunas in Colombia. *Journal of Paleontology*, 29(2), 212–225.

Premoli Silva, I., & Verga, D. (2011) P*ractical manual of Cretaceous planktonic foraminifera. New Editing by Marie Rose Petrizzo and Isabella Premoli Silva. International School on Planktonic Foraminifera 3rd Course: Cretaceous Planktonic Foraminifera*. Milano University.

Rangel, A., Parra, P., & Niño, C. (2000) The La Luna formation: chemostratigraphy and organic facies in the Middle Magdalena Basin. *Organic Geochemistry*, 31(12), 1267–1284.

Roth, P.H. (1983) Jurassic and Lower Cretaceous calcareous nannofossils in the Western North Atlantic (Site 534): biostratigraphy, preservation and some observations on biogeography and paleoceanography. *Init. Rep. DSDP*, 76, 587–621.

Santos C. E. (2012), *Palynostratigraphy of the Umir Formation, Middle Magdalena Valley Basin (MMVB) Colombia*" (MSc Theses Louisiana State University, United States). Available from / Retrieved from [https://digitalcommons.lsu.edu/gradschool_theses/2122].

Sarmiento, G. (1992). Palinología de la Formación Guaduas. Estratigráfica y Sistemática. *Boletín Geológico*, 32 (1–3), 45–126.

Sarmiento, G., Puentes, J., & Sierra, C. (2015) Evolución geológica y estratigráfica del sector norte del Valle Medio del Magdalena. *Geología Norandina*, 12, 51–82.

Sarmiento-Rojas, L.F. (2019) Cretaceous stratigraphy and paleo-facies maps of northwestern South America. In F. Cediel, & R.P. Shaw (Eds.). *Geology and Tectonics of Northwestern South America. The Pacific Caribbean Andean Junction* (pp. 673–747). Springer.

Scott, H.W., 1961. Classification of Ostracoda. Q74-Q91. In R.C. Moore, & C.W Pitrat (Eds.). *Treatise on invertebrate paleontology, Part Q, Arthropoda 3: Crustacea, Ostracoda*. Geological Society of America and University of Kansas Press.

Sellier de Civrieux, J.M. (1952) Estudio de la microfauna de la sección-tipo del Miembro Socuy de la Formación Colón, Distrito Mara, Estado Zulia. *Boletín de Geología y Minas (Venezuela)*, 2(5), 231–310.

Shenkar, N., & Swalla, B.J. (2011) Global Diversity of Ascidiacea. *PLoS ONE*, 6, e20657, DOI:10.1371/journal.pone.0020657.

678 Sole de Porta, N. (1972) Palinologia de la Formacion Cimarrona (Maastrichtiense) en el
679 valle medio del Magdalena, Colombia. *Studia Geologica*, 4, 103–142.
680 Sohn, I.G. (1961) Techniques for preparation and study of fossil ostracodes. In R.C.
681 Moore, & C.W Pitrat (Eds.). *Treatise on invertebrate paleontology, Part Q,*
682 *Arthropoda 3: Crustacea, Ostracoda* (pp. Q63–Q70). Geological Society of
683 America and University of Kansas. Press.
684 Tchegliakova, N. (1993) Los foraminíferos y los minerales antigénicos de la Formación
685 Umir (sección Quebrada La Julia, Valle Medio del Magdalena): registro de
686 laguna costera a finales del Cretácico Superior cuspidal (Maastrichtiano).
687 *Geología Colombiana*, 18, 107–117.
688 Tchegliakova, N. (1995) Los Foraminíferos de la Formación Umir (Sección Quebrada
689 La Julia): Registro del Cretáceo Superior Cuspidal (Maestrichtiano) en el Valle
690 Medio del Magdalena, Colombia. *Geología Colombiana*, 19, 109–130.
691 Tchegliakova, N. (1996) Registro de las biozonas de foraminíferos planctónicos
692 *Gansserina gansseri* y *Abathomphalus mayaroensis* (Maastrichtiano medio y
693 superior) en el extremo meridional del Valle Medio del Magdalena (Colombia,
694 Suramérica). *Geología Colombiana*, 20, 67–90.
695 Tchegliakova, N., & Mojica, J. (2001) El Senoniano de la barrera de Girardot-Guataquí,
696 Valle Alto del Magdalena, Colombia: Precisiones sobre la estratigrafía y
697 establecimiento de una zonación micropaleontológica. *Revista de la Academia*
698 *Colombiana de Ciencias Exactas, Físicas y Naturales*, 25(94), 37–75.
699 Terraza, R. (2019) “Formación La Luna”: expresión espuria en la geología colombiana.
700 In F. Etayo-Serna (Ed.). *Estudios geológicos y paleontológicos sobre el*
701 *Cretácico en la región del embalse del río Sogamoso, Valle Medio del*
702 *Magdalena* (pp. 305–362). Servicio Geológico Colombiano 23.

Valencia-Gómez, J.C., Cardona, A., Bayona, G., Valencia, V. & Zapata, S. (2020) Análisis de procedencia del registro sin-orogénico Maastrichtiano de la Formación Cimarrona, flanco occidental de la Cordillera Oriental colombiana. *Boletín de Geología*, 42(3), 171–204.

Van der Akker, T.J.H.A., Kaminski, M.A., Gradstein, F.M., & Wood, J. (2000) Campanian to Palaeocene biostratigraphy and palaeoenvironments in the Foula Sub-basin, west of the Shetland Islands, UK. *Journal of Micropalaeontology*, 19, 23–43.

Van der Hammen, T. (1954) El desarrollo de la flora colombiana en los periodos Geológicos. Maastrichtiano hasta Terciario más inferior. (Una investigación palinológica de la Formación Guaduas y equivalentes). *Boletín Geológico* 2(1), 49–106.

Van der Hammen, T. (1957) Climatic periodicity and evolution of South American Maastrichtian and Tertiary flora (a study based on pollen analysis in Colombia). *Boletín Geológico*, 5(2), 57–91.

Vergara, L.S. (1997) Stratigraphy, foraminiferal assemblages and paleoenvironments in the Late Cretaceous of the Upper Magdalena Valley, Colombia (Part I), *Journal of South American Earth Sciences,* 10(2), 111–132.

Villamil, T., & Pindell, J. (1998) Mesozoic paleogeographic evolution of northern South America. In J. Pindell, & C. Drake (Eds.). *Paleogeographic evolution and non-glacial eustacy, northern South America* (pp.238–318). SEPM Society for Sedimentary Geology 58.

Ward, D.E., Goldsmith, R., Cruz, J. & Restrepo, H. (1973) Geología de los cuadrángulos H-12 Bucaramanga y H-13 Pamplona, Departamento de Santander. *Boletín Geológico*, 21(1–3), 1–134.

Wei, W., & Algeo, T. (2020) Elemental proxies for paleosalinity analysis of ancient shales and mudrocks. *Geochimica et Cosmochimica* Acta, 287, 341–366.

Yepes, O. (2001) Maastrichtian/Danian dinoflagellate cyst biostratigraphy and biogeography from two equatorial sections in Colombia and Venezuela. *Palynology*, 25, 217–249.

Figure captions

Figure 1. 1. Location of the Middle Magdalena Valley Basin. **2.** Map showing the location of the Aguablanca Creek section, northeastern Colombia. **Abbreviations**: **CC**, Central Cordillera; **EC**, Eastern Cordillera; **UMB**, Upper Magdalena basin; **MMB**, Middle Magdalena basin; **LMB**, Lower Magdalena basin; **CB**, Catatumbo basin; **RSZ**, Romeral suture zone; **ESFS**, Espiritu Santo fault system; **BSFS**, Bituima and La Salina fault system; **BSMF**, Bucaramanga-Santa Marta fault system.

Figure 2. Stratigraphic distribution of foraminiferal taxa at Aguablanca Creek section. Biozones identification follows the local foraminiferal assemblage zones of Cushman and Hedberg (1941). Stratigraphic column based on descriptions of Terraza (2019). Gray dots indicate samples barren in foraminifers; red dashed line indicates the xenoconformity between the La Luna and Umir formations.

Figure 3. Selected foraminifers from Aguablanca Creek section. SEM Images. Scale bars represent 100 µm. **1.** *Spiroplectammina spectabilis* (337.6 m); **2.** *Haplophragmoides walteri* (334.9 m); **3.** *Ammobaculites colombiana* (343 m); **4**. *Haplophragmoides excavatum* (338.2 m); **5.** *Haplophragmoides glaber* (333.9 m); **6.**

Gaudryina quadrans (329.9 m); **7.** *Lenticulina muensteri* (337.6 m); **8.** *Lenticulina* cf. *williamsoni* (329.9 m); **9**. *Gavelinella henbesti* (334.9 m); **10-11.** *Gyroidinoides depressus* (336 m); **12.** *Marginulinopsis texasensis* (331.3 m); **13.** *Dentalina wimani* (331 m); **14.** *Stilostomella stimea* (329.9 m); **15.** *Nodosaria paupercula* (337.6 m); **16.** *Praebulimina* spp. (334.9 m); **17.** *Pyramidina prolixa* (335.5 m); **18.** *Spiroplecta americana* (336 m); **19.** *Pseudoguembelina costulata* (336.9 m); **20.** *Pseudoguembelina excolata* (330.3 m); **21.** *Siphogenerinoides bramletti* (334.9 m); **22.** *Orthokarstenia cretacea* (331.3 m); **23.** *Globotruncana aegyptiaca* (336 m); **24**. *Rugoglobigerina macrocephala* (331.3 m); **25**. *Muricohedbergella* cf. *holmdelensis* (334.9 m).

Figure 4. Stratigraphic distribution of calcareous nannofossil taxa at Aguablanca Creek section. Biozones identification follows the local foraminiferal assemblage zones of Cushman and Hedberg (1941). Stratigraphic column based on descriptions of Terraza (2019). Gray dots indicate samples barren in calcareous nannofossils; red dashed line indicates the xenoconformity between the La Luna and Umir formations.

Figure 5. Selected calcareous nannofossils from Aguablanca Creek section. Scale bar represents 5 µm for all images. Petrographic microscopy images. **1-2.** *Arkhangelskiella cymbiformis* (321.2 m); **3-4.** *Gartnerago segmentatum* (329.9 m); **5-6.** *Micula staurophora* (323.4 m); **7-8.** *Quadrum gartneri* (321.2 m); **9-10.** *Reinhardtites levis* (331 m); **11-12.** *Watznaueria barnesiae* (321.2 m); **13-14.** *Zeugrhabdotus bicrescenticus* (321.2 m); **15-16.** Ascidian spicule (340 m).

Figure 6. Records of foraminiferal and calcareous nannofossil distribution of diversity and richness estimates, and geochemical proxies at Aguablanca Creek section. **1.**

778 Species richness of foraminiferal and calcareous nannofossil assemblages. **2.** Shannon-
779 H diversity of foraminiferal and calcareous nannofossil assemblages. **3.** Ln (E)
780 estimates for calcareous nannofossil assemblages. **4.** Log (Fe/Ca) as a proxy for
781 terrigenous input. **5.** Sr/Ba ratio as a proxy for paleosalinity. **6.** Stratigraphic distribution
782 of the redox-sensitive trace metals Ni, Cu, V, and Zn normalized to Al content. Red
783 dashed line indicates the xenoconformity between the La Luna and Umir formations.
784
785 **Figure 7.** Interpreted paleoenvironmental settings of Maastrichtian successions in
786 northern South America. **1.** Paleogeographic map adapted from Bayona (2018),
787 indicating the location of the Aguablanca Creek section (AC) and additional localities
788 with foraminiferal data numbers 1-5). **2.** Depositional setting and age assignments for
789 latest Cretaceous sedimentary successions of northeastern Colombia. Age and
790 paleoenvironmental assignments follow: 1-2 Tchegliakova (1993, 1995, 1996); 3
791 Navarrete *et al.* (2018) and Pérez-Panera *et al.* (2018); 4-5 Patarroyo *et al.* (2017, 2022).
792 The horizontal length of each bar indicates the proposed depositional setting range for
793 each locality.
794
795 **Table S1.** Total foraminifer counts at Aguablanca Creek section.
796 **Table S2.** Total calcareous nannofossil counts at Aguablanca Creek section.
797 **Table S3.** Sediments geochemical data (XRF analysis) at Aguablanca Creek section.
798
799
800
801
802

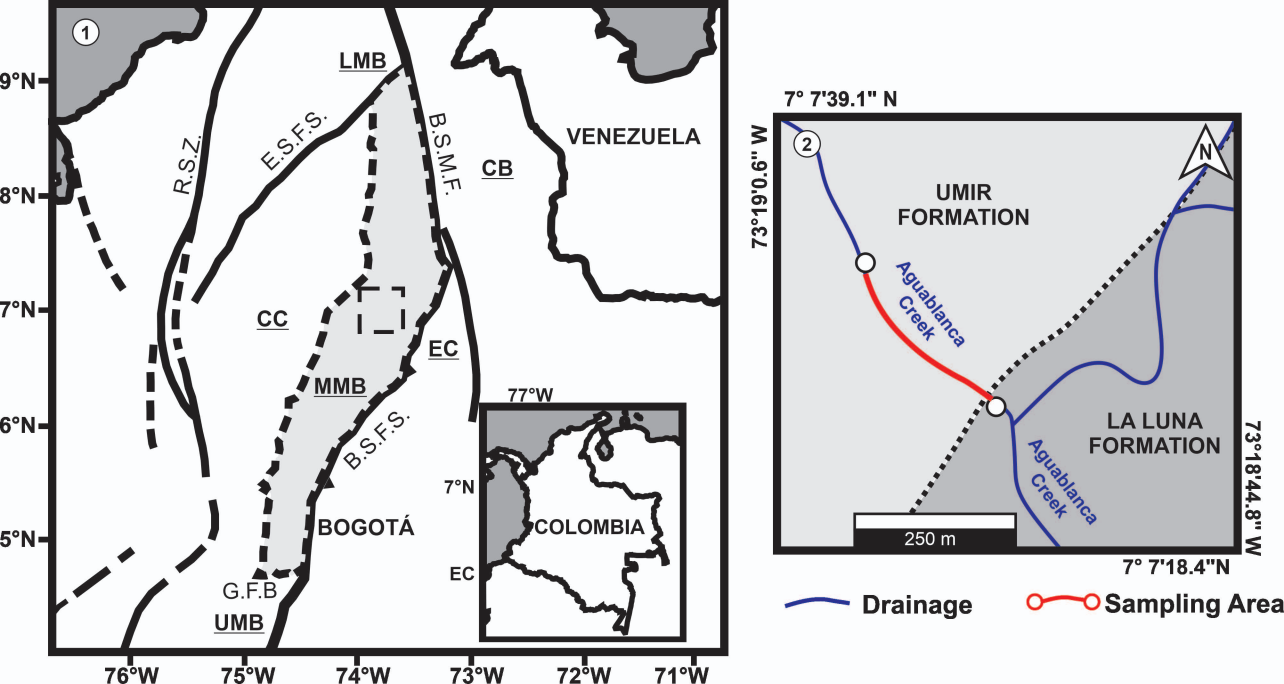
1
9°N
8°N
7°N
6°N
5°N
76°W
75°W
74°W
73°W
72°W
71°W
LMB
R.S.Z.
E.S.F.S.
B.S.M.F.
CB
VENEZUELA
CC
EC
MMB
B.S.F.S.
BOGOTÁ
G.F.B
UMB
77°W
7°N
EC
COLOMBIA
2
7° 7'39.1" N
73°19'0.6" W
UMIR
FORMATION
Aguablanca
Creek
LA LUNA
FORMATION
Aguablanca
Creek
N
250 m
73°18'44.8" W
7° 7'18.4"N
Drainage
Sampling Area

AGUABLANCA CREEK
LITHOLOGY
SAMPLES
LA LUNA FORMATION
CAMPANIAN TO EARLY MAASTRICHTIAN
UMIR FORMATION
EARLY TO LATE MAASTRICHTIAN
Not defined
Siphogenerinoides bramlettei
Ammobaculites colombiana
320 m
330 m
340 m
350 m
Archaeoglobigerina spp.
Globotruncana aegyptiaca
Muricohedbergella cf. holmdelensis
Planoheterohelix spp.
Pseudoguembelina costulata
Pseudoguembelina excolata
Rugoglobigerina macrocephala
Spiroplecta americana
Ammobaculites colombiana
Gaudryina quadrans
Haplophragmoides excavatum
Haplophragmoides glaber
Haplophragmoides walteri
Nothia robusta
Spiroplectammina spectabilis
Dentalina wimani
Gavelinella correcta
Gavelinella henbesti
Gavelinella spissocostata
Gavelinella spp.
Gyrodinoides depressa
Lagena spp.
Lenticulina muensteri
Lenticulina cf. williamsoni
Lenticulina sp2
Marginulinopsis texasensis
Nodosaria paupercula
Orthokarstenia cretacea
Praebulimina kickapoensis
Pseudoglandulina spp.
Pyramidina prolixa
Pyramidina triangularis
Siphogenerinoides bramlettei
Stilostomella spinea
Indet. Globigerinina
Indet. Textularina
Indet. Rotaliina
Ostracodes
Gastropods
Fish teeth
Phosphatic pellets
Glauconite
RARE (<2)
FEW (2-4)
COMMON (5-15)
ABUNDANT (>15)
LIMESTONES
GLAUCONITIC SANDSTONES
SILTSTONES
MUDSTONES
MARLSTONES

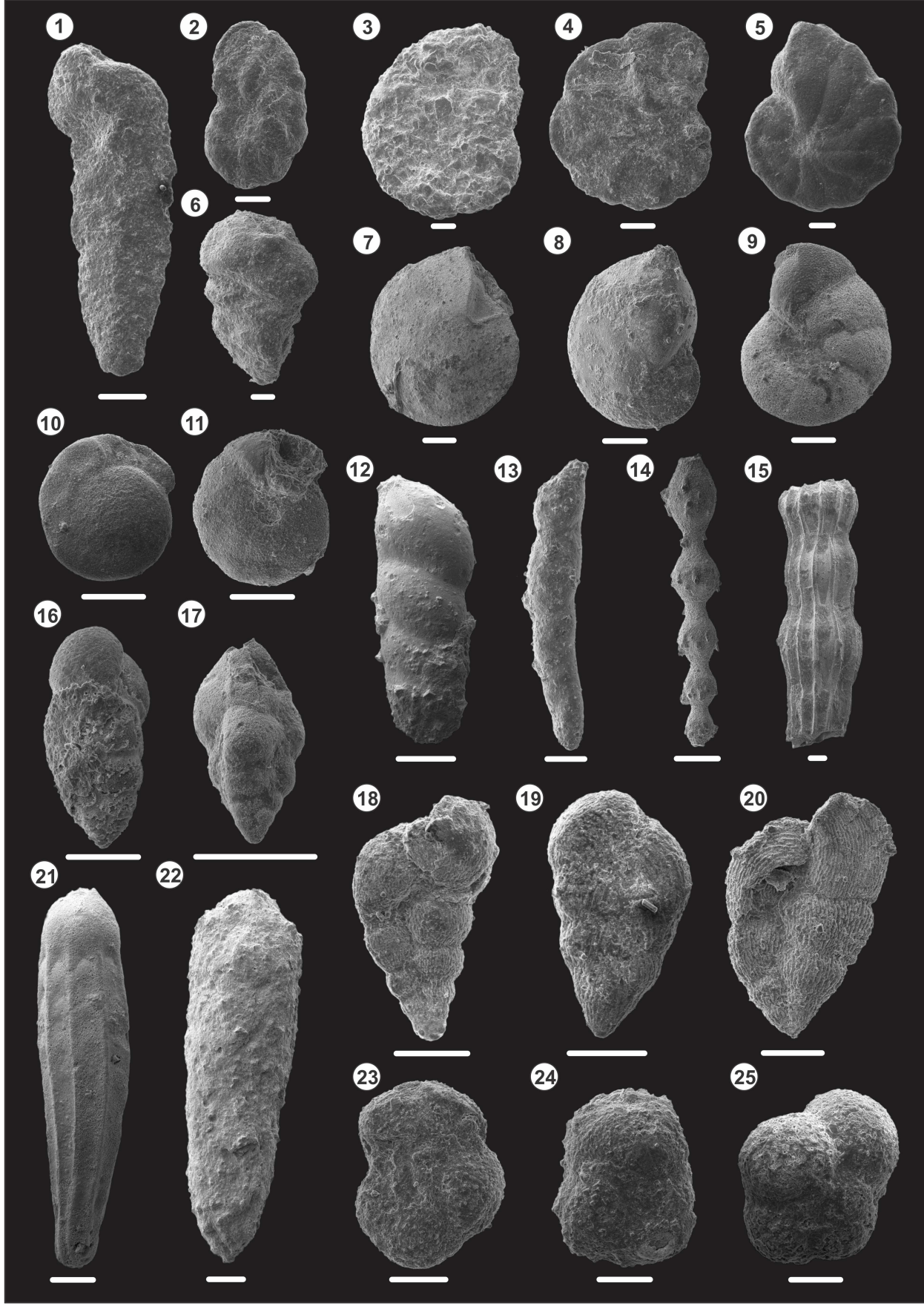
1
2
3
4
5
6
7
8
9
10
11
12
13
14
15
16
17
18
19
20
21
22
23
24
25

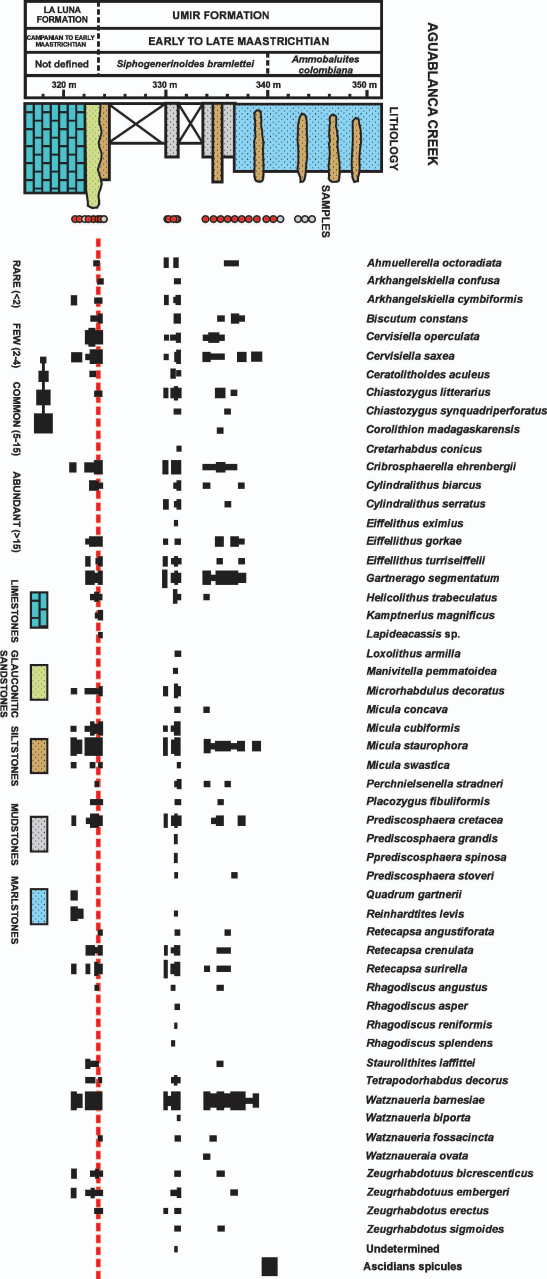
LA LUNA FORMATION
UMIR FORMATION
CAMPANIAN TO EARLY MAASTRICHTIAN
EARLY TO LATE MAASTRICHTIAN
Not defined
Siphogenerinoides bramlettei
Ammobaluites colombiana
AGUABLANCA CREEK
320 m
330 m
340 m
350 m
LITHOLOGY
SAMPLES
RARE (<2)
FEW (2-4)
COMMON (5-15)
ABUNDANT (>15)
LIMESTONES
GLAUCONITIC SANDSTONES
SILTSTONES
MUDSTONES
MARLSTONES
Ahmuellerella octoradiata
Arkhangelskiella confusa
Arkhangelskiella cymbiformis
Biscutum constans
Cervisiella operculata
Cervisiella saxea
Ceratolithoides aculeus
Chiastozygus litterarius
Chiastozygus synquadriperforatus
Corolithion madagaskarensis
Cretarhabdus conicus
Cribrosphaerella ehrenbergii
Cylindralithus biarcus
Cylindralithus serratus
Eiffelithus eximius
Eiffellithus gorkae
Eiffellithus turriseiffelli
Gartnerago segmentatum
Helicolithus trabeculatus
Kamptnerius magnificus
Lapideacassis sp.
Loxolithus armilla
Manivitella pemmatoidea
Microrhabdulus decoratus
Micula concava
Micula cubiformis
Micula staurophora
Micula swastica
Perchnielsenella stradneri
Placozygus fibuliformis
Prediscosphaera cretacea
Prediscosphaera grandis
Ppredicosphaera spinosa
Prediscosphaera stoveri
Quadrum gartnerii
Reinhardtites levis
Retecapsa angustiforata
Retecapsa crenulata
Retecapsa surirella
Rhagodiscus angustus
Rhagodiscus asper
Rhagodiscus reniformis
Rhagodiscus splendens
Staurolithites laffittei
Tetrapodorhabdus decorus
Watznaueria barnesiae
Watznaueria biporta
Watznaueria fossacincta
Watznaueraia ovata
Zeugrhabdotuus bicrescenticus
Zeugrhabdotuus embergeri
Zeugrhabdotus erectus
Zeugrhabdotus sigmoides
Undetermined
Ascidians spicules

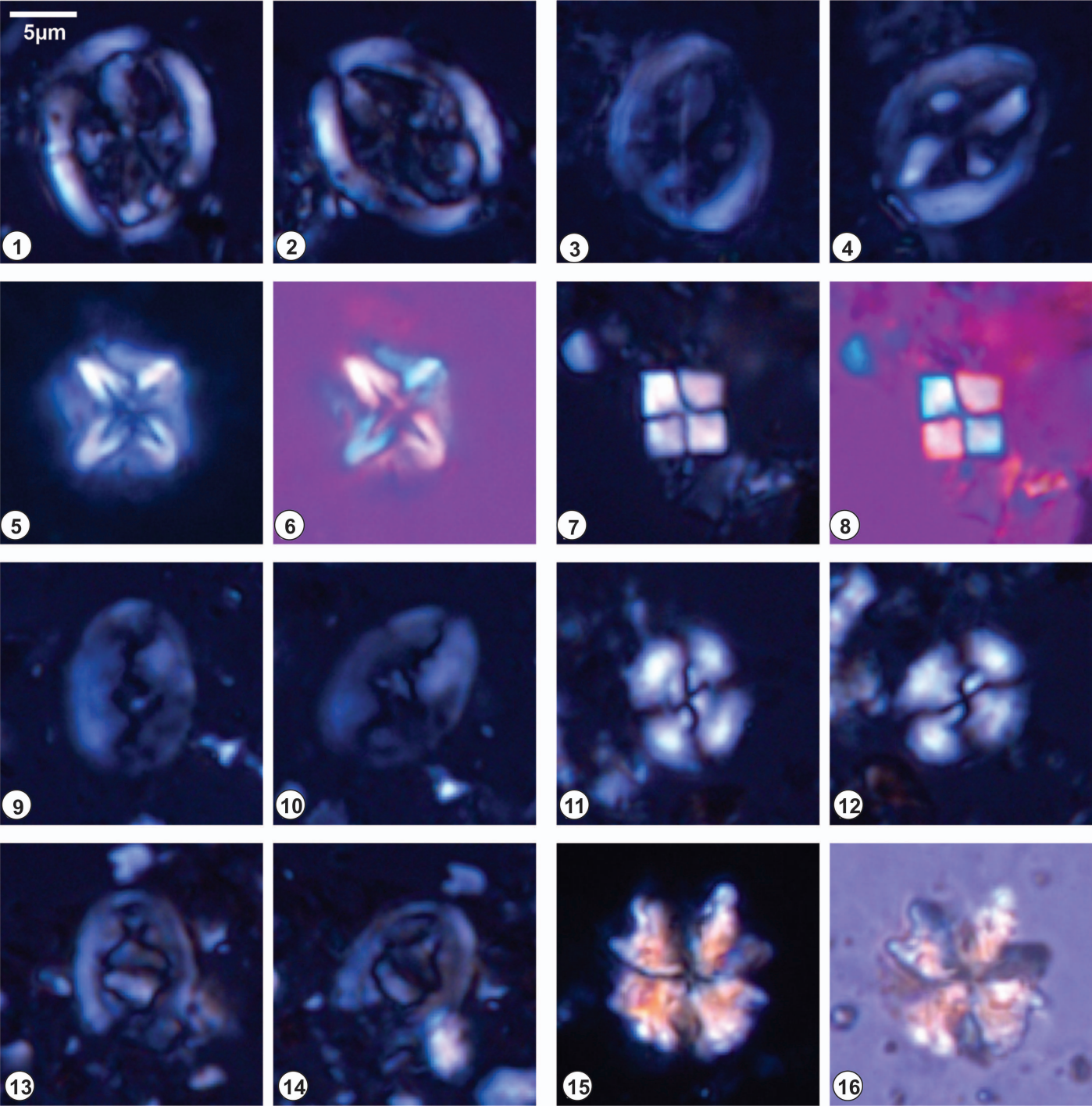
5µm
1
2
3
4
5
6
7
8
9
10
11
12
13
14
15
16

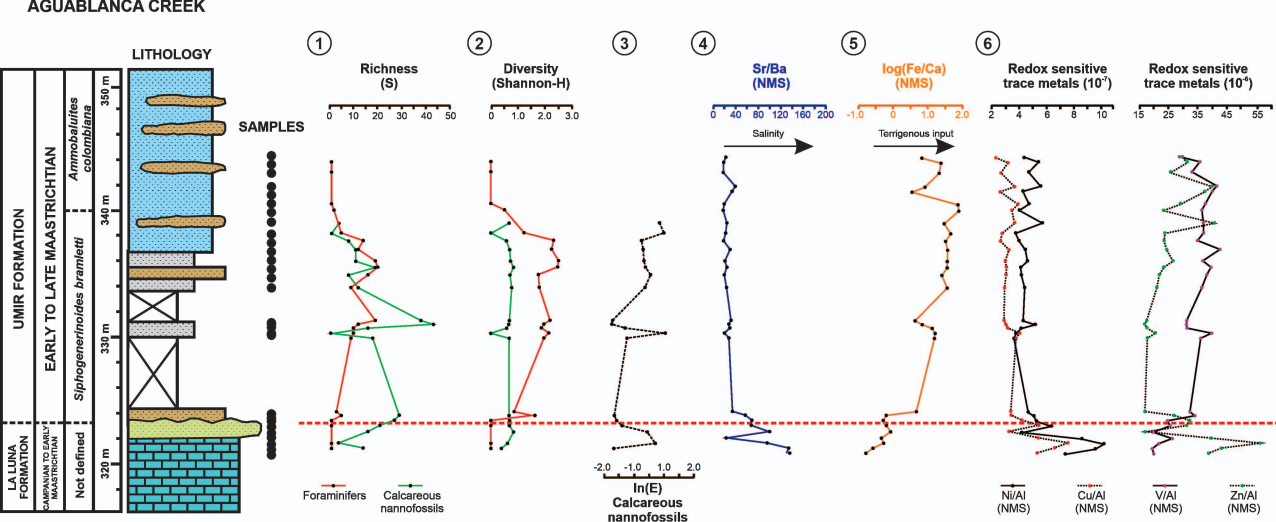
AGUABLANCA CREEK
LITHOLOGY
SAMPLES
UMIR FORMATION
EARLY TO LATE MAASTRICHTIAN
Ammobaculites colombiana
Siphogenerinoides bramlietti
LA LUNA FORMATION
CAMPANIAN TO EARLY MAASTRICHTIAN
Not defined
350 m
340 m
330 m
320 m
1
Richness (S)
0 10 20 30 40 50
2
Diversity (Shannon-H)
0 1.0 2.0 3.0
3
ln(E) Calcareous nannofossils
-2.0 -1.0 1.0 2.0
4
Sr/Ba (NMS)
0 40 80 120 160 200
Salinity
5
log(Fe/Ca) (NMS)
-1.0 0 1.0 2.0
Terrigenous input
6
Redox sensitive trace metals (10^{-7})
2 4 6 8 10
Redox sensitive trace metals (10^{-6})
15 25 35 45 55
Foraminifers
Calcareous nannofossils
Ni/Al (NMS)
Cu/Al (NMS)
V/Al (NMS)
Zn/Al (NMS)

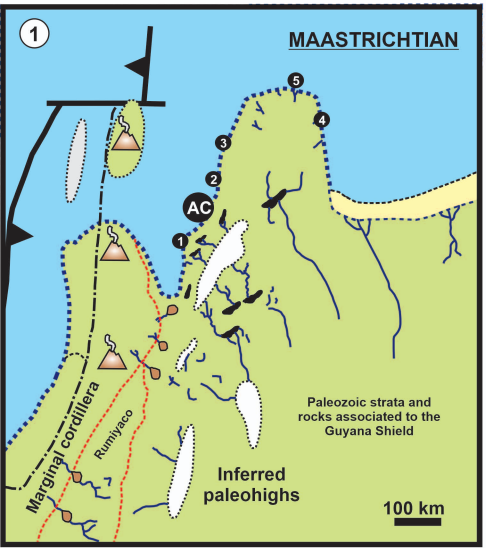
1
MAASTRICHTIAN
5
4
3
2
AC
1
Paleozoic strata and rocks associated to the Guyana Shield
Marginal cordillera
Rumiyaco
Inferred paleohighs
100 km

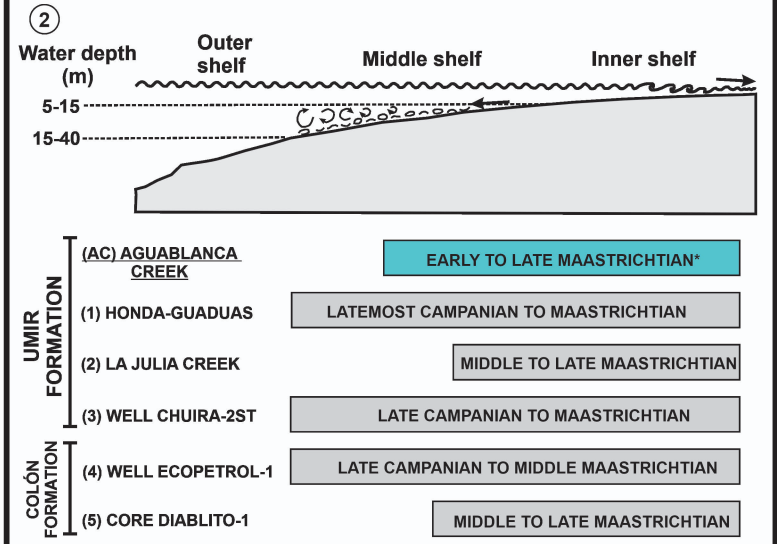
2
Water depth (m)
Outer shelf
Middle shelf
Inner shelf
5-15
15-40
UMIR FORMATION
(AC) AGUABLANCA CREEK
EARLY TO LATE MAASTRICHTIAN*
(1) HONDA-GUADUAS
LATEMOST CAMPANIAN TO MAASTRICHTIAN
(2) LA JULIA CREEK
MIDDLE TO LATE MAASTRICHTIAN
(3) WELL CHUIRA-2ST
LATE CAMPANIAN TO MAASTRICHTIAN
COLÓN FORMATION
(4) WELL ECOPETROL-1
LATE CAMPANIAN TO MIDDLE MAASTRICHTIAN
(5) CORE DIABLITO-1
MIDDLE TO LATE MAASTRICHTIAN